JACS
JOURNAL OF THE AMERICAN CHEMICAL SOCIETY
Article
pubs.acs.org/JACS

Cerium(IV) Imido Complexes: Structural, Computational, and Reactivity Studies

Lukman A. Solola, Alexander V. Zabula, Walter L. Dorfner, Brian C. Manor, Patrick J. Carroll, and Eric J. Schelter*

P. Roy and Diana T. Vagelos Laboratories, Department of Chemistry, University of Pennsylvania, 231 South 34th Street, Philadelphia, Pennsylvania 19104, United States

Supporting Information

ABSTRACT: A series of alkali metal capped cerium(IV) imido complexes, $[M(solv)_x][Ce{=}N(3,5\text{-}(CF_3)_2C_6H_3)(TriNOx)]$ (M = Li, K, Rb, Cs; solv = TMEDA, THF, Et_2O, or DME), was isolated and fully characterized. An X-ray structural investigation of the cerium imido complexes demonstrated the impact of the alkali metal counterions on the geometry of the $[Ce{=}N(3,5\text{-}(CF_3)_2C_6H_3)(TriNOx)]^-$ moiety. Substantial shortening of the Ce=N bond was observed with increasing size of the alkali metal cation. The first complex featuring an unsupported, terminal multiple bond between a Ce(IV) ion and a ligand fragment was also isolated by encapsulation of a Cs^+ counterion with 2.2.2-cryptand. This complex shows the shortest recorded Ce=N bond length of 2.077(3) Å. Computational investigation of the cerium imido complexes using DFT methods showed a relatively larger contribution of the cerium 5d orbital than the 4f orbital to the Ce=N bonds. The $[K(DME)_2][Ce{=}N(3,5\text{-}(CF_3)_2C_6H_3)(TriNOx)]$ complex cleaves the Si—O bond in $(Me_3Si)_2O$, yielding the $[(Me_3SiO)Ce^{IV}(TriNOx)]$ adduct. The reaction of the rubidium capped imido complex with benzophenone resulted in the formation of a rare Ce(IV)−oxo complex, that was stabilized by a supramolecular, tetrameric oligomerization of the Ce=O units with rubidium cations.

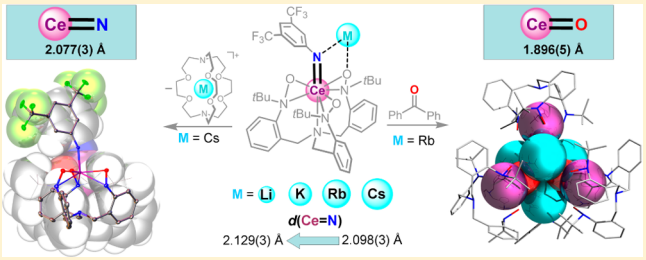

INTRODUCTION

Significant progress has been made in the study of complexes possessing transition metal−ligand multiple bonds in natural and synthetic systems, elucidation of their electronic structures, and the investigation of their unique reactivities.[1] These studies have culminated in the application of such compounds as catalysts for various transformations in synthetic organic and industrial chemistry.[2] Likewise, there has been a resurgence in the study of actinide−ligand multiple bonds.[3] Such actinide complexes have been synthesized using several routes including trityl deprotection,[3c] aryl azide reduction,[3d] and reductive cleavage of nitrite.[3g] However, the chemistry of complexes containing multiple bonds between rare-earth (RE) metals and main group elements is still in its infancy.[4] Multiply bound RE=E (E = O, N, P) moieties are expected to be less acidic and more reactive than their transition metal analogues due to their stronger bond polarization. Indeed, the rarity of RE=E complexes can be attributed to energy mismatch between valence metal and ligand orbitals,[4a,b] which is responsible for the strong polarization of the RE=E bond. In addition, the Lewis acidity of lanthanide ions and nondirectional nature of Ln—E bonding often result in oligomerization of the corresponding complexes upon formation.[4b,5]

Despite the above-mentioned challenges, a handful of RE=E complexes have been reported and their reactivities studied. Mindiola and co-workers provided evidence to support the generation of a complex bearing a Sc=N bond as an intermediate.[6] Chen and co-workers isolated the first Sc=N complex by deprotonation of a scandium anilide complex.[7] A similar synthetic route was later employed by Mindiola and co-workers for the isolation of a Sc=P complex, supported by an "-ate" interaction.[8] The reactivity of this complex was explored, and a putative Sc=O complex was proposed as an intermediate in its reaction with benzophenone. Anwander and co-workers have recently prepared the first terminal lanthanide−imido complex **I** (Scheme 1) featuring a trivalent lutetium ion.[9]

Scheme 1. Selected Complexes Bearing Rare Earth Metal−Ligand Multiple Bonds

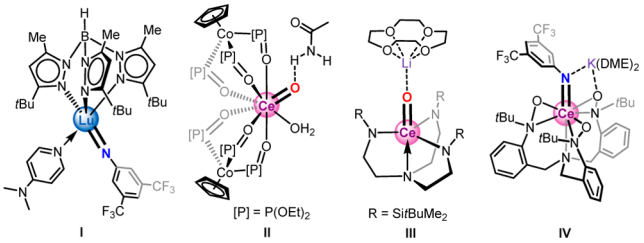

Received: November 30, 2016
Published: January 11, 2017

DOI: 10.1021/jacs.6b12369
J. Am. Chem. Soc. 2017, 139, 2435−2442

It is expected that a tetravalent lanthanide ion would provide a better electrostatic stabilization for anionic ligands, and be more capable of forming multiple bonds. Also, accessing the tetravalent state of a lanthanide ion should lower the energy of its 5d orbital, thereby leading to favorable overlap with ligand valence 2p orbitals. Indeed, it has been shown by DFT calculations that lanthanide 5d orbitals play a significant role in stabilizing Ln=E bonds.[4f] Moreover, a significant 4f orbital participation of the tetravalent cerium ion was recently established for $[CeCl_6]^{2-}$ by XAS spectroscopy,[10] and larger metal 4f orbital character was observed in $[CeCl_6]^{2-}$ than 5f in $[UCl_6]^{2-}$, suggesting that the rich metal−ligand multiple bond chemistry observed for U(IV)[11] may similarly be accessible with Ce(IV).

The above-mentioned spectroscopic and computational data are now supported by a few recent reports on the successful isolation of Ce^{IV}=E complexes. The first Ce^{IV}=O complex **II** was isolated by Leung and co-workers using a salt metathesis route,[12] and an investigation of its reactivity showed that it possessed noteworthy nucleophilic, oxidizing, and Brønsted basic properties. A stable sodium capped Ce^{IV}=O complex was also isolated.[13] Most recently, Hayton and co-workers reported the isolation of the lithium capped Ce^{IV}=O complex **III** supported by the Tren ligand framework.[14] Liddle and co-workers also recently reported the isolation of a cerium nucleophilic carbene complex with a formulation suggestive of a multiple bond between a Ce^{IV} ion and a carbon atom.[15] However, the latter assertion has proven controversial.[16]

We recently reported the synthesis of the first Ce^{IV}=N—R complex, $[K(DME)_2][(TriNOx)CeN(3,5\text{-}(CF_3)_2C_6H_3)]$ (**IV**, Scheme 1).[17] The stability of this complex was attributed to the nitroxide-based $TriNOx^{3-}$ ligand framework, which provided both electronic and steric stabilization.[18] The presence of the electron withdrawing $3,5\text{-}(CF_3)_2C_6H_3$ substituent also provides stabilization of the tetravalent cerium ion by reducing the electron density at the imido nitrogen atom in **IV**. Examination of the molecular structure of **IV** in the solid state showed the shortest known Ce—N bond length of 2.119(3) Å. The Ce=N bond was clearly polarized, with predominantly nitrogen character for the relevant orbitals involved in bonding, as determined by density functional theory (DFT). Inspired by these initial results, herein we report the impact of other alkali metal cations on the nature of the Ce=N bond, the synthesis of the first uncapped Ce^{IV}−imido complex, and initial exploration of the unusual reactivity of the Ce=N—R unit.

RESULTS AND DISCUSSION

We hypothesized that smaller and higher charge density alkali metal ions would interact strongly with the $Ce{=}N_{imido}$ core, thereby weakening the Ce=N bond. In order to investigate the role of counterions, we prepared a series of TriNOx-based Ce^{IV}=N imido complexes with the lighter (Li) and heavier (Rb and Cs) ions. These complexes (**2-M$_{solv}$**) were prepared by the deprotonation of anilide complex **1** by an appropriate alkali metal amide (Scheme 2).

^{1}H NMR monitoring for the reaction mixtures showed the generation of the imido complexes in 80% conversion within 1 h. We also determined that the *in situ* generation of the imido complexes was an appropriate approach for the studies of their reactivities (*vide infra*). Crystalline compounds **2-M$_{solv}$** were isolated as dark purple solids in low yields upon layering of their solutions with hexanes at −25 °C. The low isolated yields for complexes **2-M$_{solv}$** were due to their high solublities in common organic solvents including pentane. Similarly, despite multiple trials, it has not been possible to obtain crystalline samples of a sodium congener of **2-M$_{solv}$**.

Scheme 2. Preparation of 2-M$_{solv}$

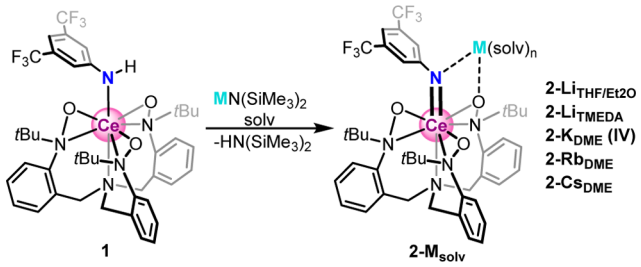

Lithium adducts of the Ce−imido complex were isolated with THF/Et_2O (1:1) or TMEDA molecules coordinated to the alkali metal ion (**2-Li$_{THF/Et2O}$** and **2-Li$_{TMEDA}$**, respectively). X-ray diffraction studies revealed the lithium ions saturated by the coordination of two O- or N-donor functionalities (Figure 1). The $Li(1)—O_{TriNOx}$ and Li(1)—N(5) distances were elongated in **2-Li$_{THF/Et2O}$** (1.962(10) and 2.021(11) Å, respectively) compared to the **2-Li$_{TMEDA}$** adduct (1.899(6) and 1.973(7) Å, respectively). The Ce(1)=N(5) bond lengths were effectively equivalent in both adducts at 2.126(4) and 2.129(3) Å and slightly elongated compared to the related

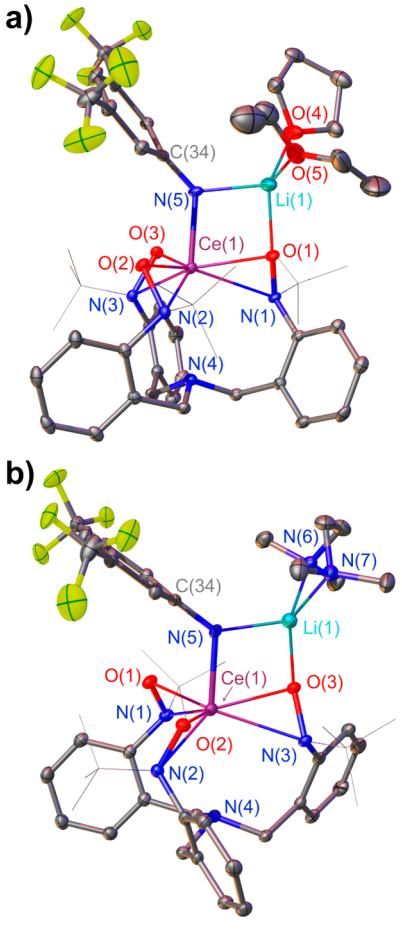

Figure 1. Thermal ellipsoid plot of **2-Li$_{THF/Et2O}$** (a) and **2-Li$_{TMEDA}$** (b) shown at the 30% probability level. Hydrogen atoms and minor disorder components have been omitted for clarity. *t*-Butyl groups are depicted using a wire frame model.

DOI: 10.1021/jacs.6b12369
J. Am. Chem. Soc. 2017, 139, 2435−2442

Ce=N bond in the potassium capped complex **2-K$_{DME}$** (2.119(3) Å, Table 1).[17] The coordination of lithium ions to the [Ce=N(3,5-(CF$_3$)$_2$C$_6$H$_3$)(TriNOx)]$^-$ unit resulted in larger deviation of the angle Ce(1)—N(5)—C(34) (133.7(3)°) in **2-Li$_{THF/Et2O}$** and 125.4(2)° in **2-Li$_{TMEDA}$** from 180° compared to the potassium complex (144.0(3)°). The smaller angles observed in the lithium complexes can be understood by noting a stronger coordination of the smaller and higher charge density lithium cation compared to the potassium cation. The difference of the Ce(1)—N(5)—C(34) angles between the lithium complexes can be attributed to crystal packing forces.

Crystallization of an anionic Ce^{IV}–imido complex with the larger alkali metal counterions, rubidium or cesium, from DME solutions resulted in the formation of the contact ion pairs [M(DME)$_2$][Ce=N(3,5-(CF$_3$)$_2$C$_6$H$_3$)(TriNOx)] (M = Rb (**2-Rb$_{DME}$**) and Cs (**2-Cs$_{DME}$**)). Both salts were found to be isostructural with essentially the same molecular conformations (Figures S1 and 2). X-ray diffraction studies for **2-Rb$_{DME}$** and **2-Cs$_{DME}$** similarly revealed the binding of the alkali metal cation to the N(5) imido and O$_{TriNOx}$ atoms in a similar fashion as observed for the lithium and potassium analogues.

Two DME molecules were coordinated to the Rb$^+$ or Cs$^+$ ions in a chelating mode. In contrast to the related potassium salt **2-K$_{DME}$**, the larger size of the alkali metal cation in **2-Rb$_{DME}$** and **2-Cs$_{DME}$** resulted in an additional intramolecular η^2-interaction between the alkali metal ion and the adjacent π-system of the 3,5-(CF$_3$)$_2$C$_6$H$_3$ substituent (Figure 2b). The corresponding M···C contacts (3.381(2)/3.494(2) Å for **2-Rb$_{DME}$** and 3.454(3)/3.532(3) Å for **2-Cs$_{DME}$**) are close to the values previously reported for Rb- or Cs-arene adducts.[19] The coordination sphere of the alkali metal cation is completed by two intermolecular M···F interactions with the neighboring CF$_3$ group. These M···F contacts, measured at 3.177(2)/3.494(2) Å for **2-Rb$_{DME}$** and 3.292(2)/3.470(3) Å for **2-Cs$_{DME}$**, lead to a 1D polymeric arrangement of the cation and anion pair in the crystal lattice (Figure 2b). Complex **2-Rb$_{DME}$** exhibits the shortest Ce^{IV}—N bond, Ce(1)=N(5) 2.098(2) Å, within the series of alkali metal ion capped complexes. The Ce(1)—N(5)—C(34) angle of 150.78(15)° in **2-Rb$_{DME}$** is larger compared to the salts with lighter alkali metal ions that range from 125.4(2) to 144.0(3)° and closer to the value of 177.5° computed using DFT in our previous report for an uncapped complex.[17] Notably, the Ce=N$_{imido}$ bond length in **2-Cs$_{DME}$** of 2.111(2) Å is slightly longer than that in **2-Rb$_{DME}$**, 2.098(2) Å. This disparity is again attributed to crystal packing forces. Key geometrical parameters for **2-Rb$_{DME}$** and **2-Cs$_{DME}$** are summarized in Table 1.

After successful isolation of the **2-M$_{solv}$** complexes, we targeted the synthesis of a Ce^{IV}–imido complex with an unsupported Ce^{IV}=N moiety, without contact stabilization by an alkali metal center. Such a complex enables the study of "pure" Ce^{IV}=N bonding. We found that a one-pot reaction involving the anilide complex **1**, CsN(SiMe$_3$)$_2$, and 2.2.2-cryptand in 1,2-difluorobenzene formed the purple complex [Cs(2.2.2-cryptand)][(TriNOx)Ce=N(3,5-(CF$_3$)$_2$C$_6$H$_3$)] (**3**). Complex **3** represents the first example of an unsupported Ce(IV)–imido complex and a rare example of an uncapped rare earth metal ligand multiple bond. In contrast to adducts **2-M$_{solv}$**, complex **3** is thermally unstable and undergoes a complete decomposition at 20 °C within 2 days in solution to as yet unidentified products. Single crystal X-ray analysis of **3**

Table 1. Experimental Geometrical (in Å and in deg) and Calculated (B3LYP/6-31G*) Parameters for 1, 2-M$_{solv}$, and 3

	Ce(1)–N(5)[a]		Ce(1)–NO$_{TriNOx}$		Ce(1)–O$_{TriNOx}$		Ce(1)–N(4)		M(1)–N(5)		Ce(1)–N(5)–C(34)	
	exp.	calcd	exp.	calcd	exp.	calcd	exp.	calcd	exp.	calcd	exp.	calcd
1	2.379(3)	2.328	2.510(3)–2.541(3)	2.619–2.632	2.158(3)–2.203(2)	2.196–2.209	2.934(3)	3.066			143.3(2)	140.9
2-Li$_{TMEDA}$	2.129(3)	2.099	2.571(3)–2.630(4)	2.664–2.331	2.219(2)–2.298(2)	2.219–2.331	3.072(3)	3.228	1.972(7)	1.992	125.4(2)	133.1
2-Na$_{DME}$[17]		2.082		2.672–2.734		2.225–2.309		3.274		2.395		146.9
2-K$_{DME}$[17]	2.119(3)	2.069	2.620(3)–2.640(3)	2.683–2.740	2.231(3)–2.277(2)	2.232–2.306	3.138(3)	3.336	2.732(3)	2.809	144.0(3)	161.5
2-Rb$_{DME}$	2.098(2)	2.065	2.613(2)–2.650(2)	2.684–2.757	2.239(2)–2.269(1)	2.243–2.306	3.183(2)	3.360	2.957(2)	3.044	150.8(9)	167.5
2-Cs$_{DME}$	2.111(2)	2.064	2.623(2)–2.642(2)	2.687–2.760	2.241(2)–2.268(2)	2.233–2.304	3.167(2)	3.360	3.091(2)	3.273	151.7(2)	170.3
3	2.077(3)	2.029	2.622(3)–2.705(4)	2.761–2.771	2.224(3)–2.265(3)	2.267–2.270	3.335(3)	3.507			157.3(4)	177.5

[a]For assignment of atoms, see Figures 1–3.

DOI: 10.1021/jacs.6b12369
J. Am. Chem. Soc. 2017, 139, 2435–2442

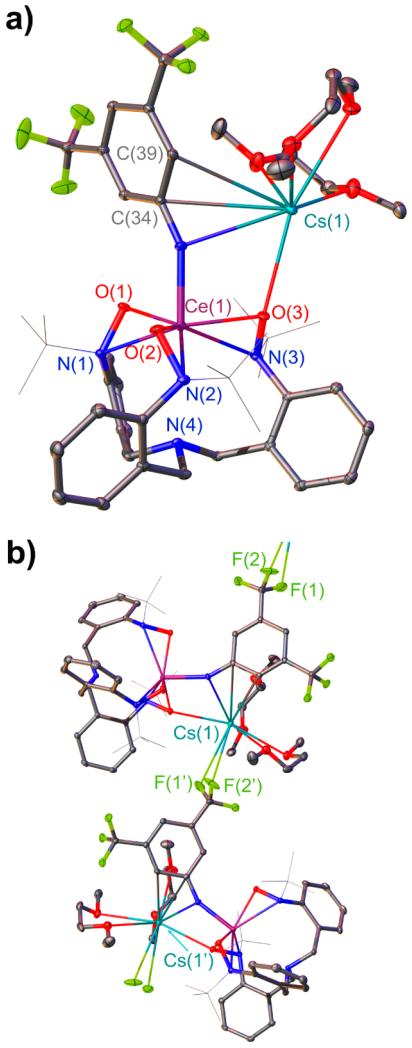

Figure 2. Thermal ellipsoid plot of **2-Cs$_{DME}$** (a) and the fragment of its polymeric arrangement (b) shown at the 30% probability level. Hydrogen atoms have been omitted for clarity. *t*-Butyl groups are depicted using a wire frame model.

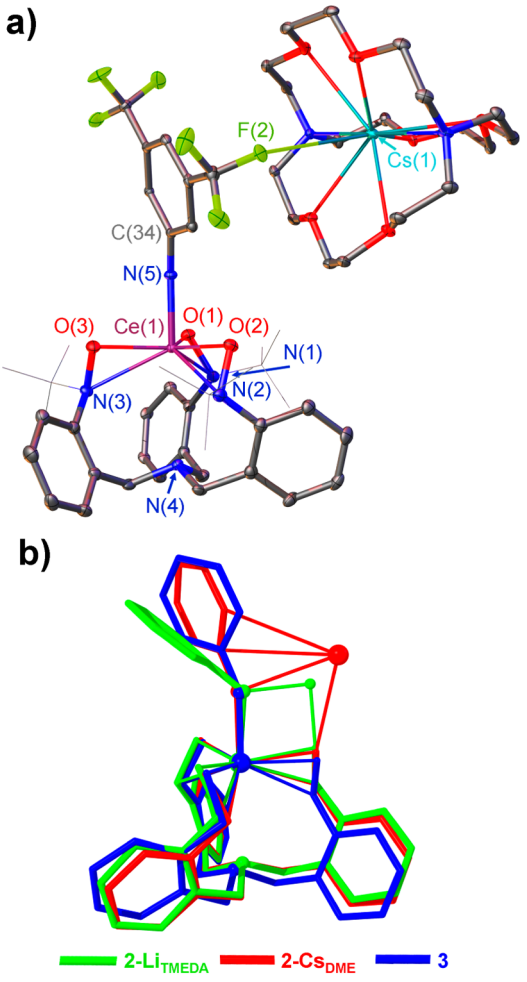

Figure 3. Thermal ellipsoid plot of **3** shown at the 30% probability level (a, *t*-butyl groups are depicted using a wire frame model); superposition of experimental geometries for **2-Li$_{TMEDA}$**, **2-Cs$_{DME}$**, and **3** (b, *t*-butyl, CF_3 groups, $[(2.2.2\text{-cryptand})Cs]^+$ cation, and solvent molecules are not shown). Hydrogen atoms have been omitted for clarity.

revealed encapsulation of the Cs^+ cation within the cryptand cavity (Figure 3a).

The Cs^+ ion also weakly interacts with the F(2) atom of the adjacent CF_3 group (3.599(3) Å). The Ce(1)═N(5) bond length (2.077(3) Å) in **3** is shorter than analogous distances measured for **2-M$_{solv}$** (2.098(2)−2.129(3) Å) and represents the shortest known Ce—N bond length. This bond length is comparable to the previously reported Lu═N bond length of 1.993(5) Å[9] after accounting for the difference in ionic radii between an eight-coordinate Ce^{IV} cation and a six-coordinate Lu^{III} cation.[20]

The Ce═N bond length in **3** is slightly longer than the reported U^{IV}═N distances in corresponding actinide complexes $K\{U(=NCPh_3)[N(SiMe_3)_2]_3\}$ (1.9926(14) Å),[3f] $[K(C_6H_6)][((ArO)_3tacn)U^{IV}(=NCPh_3)]$ (2.036(2) Å, $(ArO)_3tacn$ = trianion of 1,4,7-tris(2-hydroxy-5-methyl-3-neopentylbenzyl)-1,4,7-triazacyclononane),[11d] and $U(=NtBu)I_2(tBu_2bpy)(THF)_2$ (1.981(2) Å).[11f] The Ce(1)—N(5)—C(34) bond angle in **3** (157.3(3)°) is the largest in the corresponding series (Figure 3b, Table 1). Conversely, the Ce(1)—N(4) bond length to the bridgehead amine in **3** (3.335(3) Å) represents the longest in the series of imido complexes and indicates an increased interaction between the cerium and imido nitrogen atom.

The ^1H NMR spectra of the alkali metal capped complexes, **2-M$_{solv}$**, exhibit noticeable differences for the $\delta(^1H)$ chemical shifts of the CH_2 and 3,5-$(CF_3)_2C_6H_3$ units compared to those measured in the ^1H NMR spectrum of **3** (Figure 4). This observation can be explained by the persistence of alkali metal coordination in the solutions of **2-M$_{solv}$**. The most distinct differences in chemical shifts were observed for the ^1H NMR spectrum of **2-Li$_{TMEDA}$** that is in agreement with the strongest binding of alkali metal cation in the lithium adduct compared to its heavier homologues. The ^7Li NMR spectra for **2-Li$_{TMEDA}$** (THF-d_8) measured in a temperature range from 20 to −80 °C showed only one sharp resonance centered at 2.50 ppm (Figure S2, Supporting Information). The ^{133}Cs NMR spectrum of **2-Cs$_{DME}$** measured in the temperature range from 30 to −80 °C in THF-d_8 shows a resonance signal at δ = −8.2 ppm (Figure S3, Supporting Information). The ^{133}Cs resonance signal for **3** appears at δ = 244 ppm (THF-d_8) at temperatures below −70 °C. This value of $\delta(^{133}Cs)$ is nearly identical to that previously reported for an inclusive form of the $[Cs(2.2.2\text{-cryptand})]^+$ cation (δ = 240 ppm).[21]

DOI: 10.1021/jacs.6b12369
J. Am. Chem. Soc. 2017, 139, 2435−2442

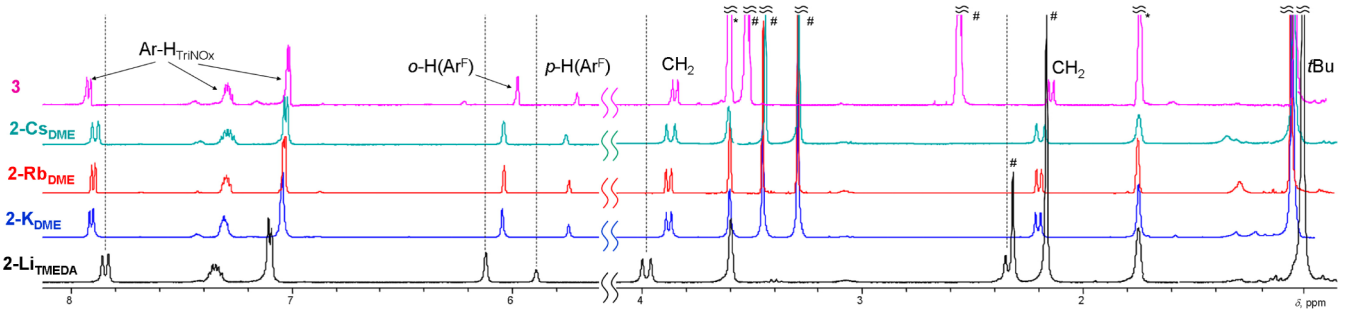

Figure 4. ^{1}H NMR spectra for **2-M$_{solv}$** and **3** in THF-d_8 (* - proteo solvent peaks, # - TMEDA, DME, or 2.2.2-cryptand signals).

Cyclic voltammetry measurements for **2-M$_{solv}$** and **3** exhibited reversible Ce$^{III/IV}$ couples in a narrow range from −1.39 to −1.41 V versus an internal Fc/Fc$^+$ standard (Figure 5a). One low intensity quasi-reversible reduction wave at E_{pc} = −2.07 V was observed in the cyclic voltammogram of **2-Li$_{TMEDA}$** (Figure S10, Supporting Information). This feature was assigned to one-electron donation into the π^* orbital of the imido aryl ring. The UV−vis spectra for **2-Li$_{TMEDA}$** showed an absorbance band at λ_{max} = 519 nm (Figure 5b). For its heavier analogues and **3**, this band was hypsochromically shifted to λ_{max} = 510−513 nm. The broad and low energy transitions measured in the electronic absorption spectra of **2-M$_{solv}$** and **3** are consistent with ligand to metal charge transfer for an f^0 Ce(IV) ion.[22]

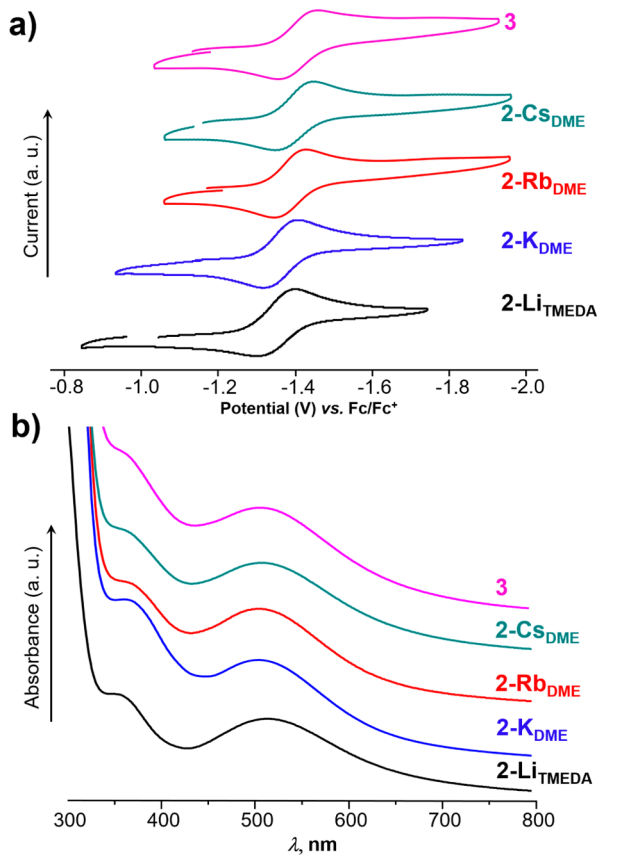

Figure 5. Isolated cerium(III/IV) redox couples (a, 1.0 mM in DME, 100 mV/s, 0.1 M [nPr$_4$N][B(3,5-(CF$_3$)$_2$C$_6$H$_3$)$_4$]) and UV−vis spectra (b, THF) of **2-M$_{solv}$** and **3**.

Computational Studies. Previously, we used DFT calculations (B3LYP/6-31G*) to understand the nature of the Ce−N$_{anilide/imido}$ bonding interactions in complexes **1**, **2-K$_{DME}$**, and **3′** (complex **3** without the Cs(2.2.2-cryptand)$^+$ counterion).[17] Our investigations showed increasing contributions of the cerium 4f and 5d orbitals to bonding with shortening of the Ce−N bond. For the current work, these calculations have been expanded to include the full series of alkali metal capped Ce(IV)−imido complexes, including the putative sodium complex **2-Na$_{DME}$**. There was a general agreement between the key geometrical indices in the computed (gas phase) and X-ray structures. However, the computationally determined Ce(1)−N(5) bond lengths in **1**, **2-M$_{solv}$**, and **3′** were consistently slightly underestimated compared to the experimentally determined values (Table 1). Also, the Ce−N$_{imido}$−C$_{ipso}$ bond angles determined experimentally were smaller by 7.7−20.3° than the computed values.

Our initial DFT results showed a difference between **2-K$_{DME}$** and the putative uncapped imido complex, **3′**. For example, the computed Mayer bond orders (MBOs) for **2-K$_{DME}$** and **3′** were different by 0.18. The calculated Ce═N bond distance in **3′** was also 0.04 Å shorter than that calculated for **2-K$_{DME}$**. These observations indicated a weak interaction of the potassium cation to the Ce═N bond.

Further evidence to support our assertion that the larger alkali metal cations were weakly associated with the imido core was provided upon examination of the Mayer bond orders (MBOs) of the Ce═N bond in the series of complexes. As expected, an increase in the MBOs of the Ce—N$_{imido}$ was observed with weakening of the interaction between the alkali metal and the imido nitrogen atom. An MBO of 1.19 was observed for complex **2-Li$_{TMEDA}$** which supports experimental observations that the Li$^+$ cation interacts the strongest with the imido core in the series (Figure 6a). Complex **2-Na$_{DME}$** had an intermediate MBO of 1.39, while **2-(K-Cs)$_{DME}$** had essentially similar MBO values ranging from 1.52 to 1.59. There was a significant difference between the MBO of the imido complexes with larger capping alkali metals (K$^+$, Rb$^+$, and Cs$^+$) and the uncapped imido complex **3′** (1.70).

As observed in complex **2-K$_{DME}$**, the Ce═N$_{imido}$ bond can be described as strongly polarized with the imido nitrogen having the major contribution to bonding across the series. As shown in Figure 6d and Table S1, the contribution of cerium to the σ-type bond increased across the series from 10.4% for anilide **1** to 13.8% for the charge separated imido anion **3′**. Similarly, there was an increase in the contribution of the cerium ion to the π-type bond from 17.3% for **2-Li$_{TMEDA}$** to 19.6% for **3′** (Figure 6e). A breakdown of the Ce bonding orbitals showed that the 5d orbital was the major contributor to bonding across the series. However, the contribution of the 4f orbital increased

DOI: 10.1021/jacs.6b12369
J. Am. Chem. Soc. 2017, 139, 2435−2442

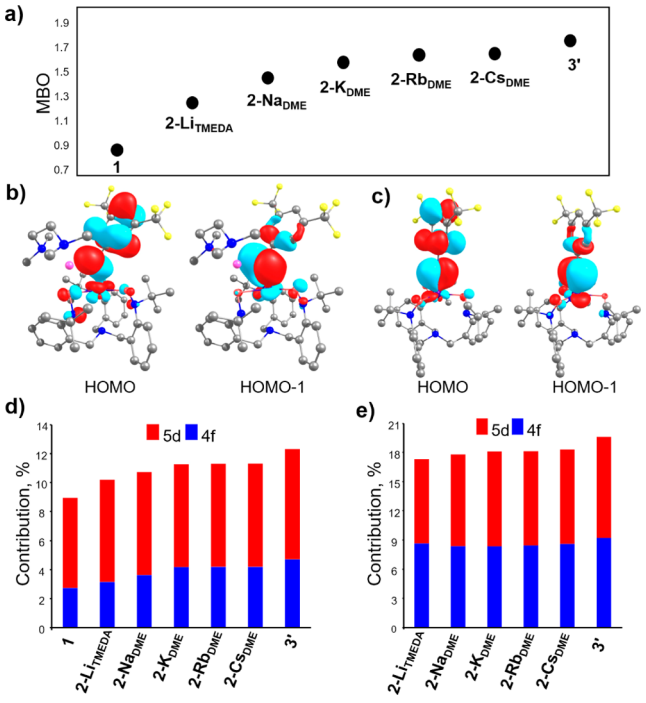

Figure 6. Calculated MBOs (a); plots of the Kohn–Sham orbitals, HOMO and HOMO−1, for **2-Li$_{TMEDA}$** (b) and **3′** (c); contributions of 5d and 4f orbitals of the Ce ion into the σ- (d) and π- (e) bonding of Ce(1)–N(5) in **1**, **2-M$_{solv}$**, and **3′**.

steadily in the σ-bonding interactions across the series from anilide **1** to the charge separated imido anion (27 to 34%). These results suggest that 4f orbital participation in covalent interactions is enhanced with increasing, uncompensated negative charge on the imido nitrogen atom. These data are also consistent with previous observations by XAS spectroscopy about the increased role played by the 4f orbitals of the cerium ion in $[CeCl_6]^{2-}$ in covalent interactions.[10]

Reactivity Studies. The polarization of the Ce═N bond renders the imido fragment strongly nucleophilic. Our preliminary reactivity studies showed that complex **2-K$_{DME}$** reacted readily with Me_3SiCl to give a Ce(IV)–amide complex.[17] Complex **2-K$_{DME}$**, generated *in situ*, also readily cleaved a strong and unreactive Si—O bond in $(Me_3Si)_2O$ to give Ce(TriNOx)OSiMe$_3$ (**4**) in a yield of 90% under ambient conditions (Figure 7a). The byproduct of this reaction, $KN(SiMe_3)(3,5\text{-}(CF_3)_2C_6H_3)$, was identified by comparing ^{1}H and ^{19}F NMR spectra of the reaction mixture with NMR spectra, obtained for the independently prepared substrate (Figure S4). Red crystals of **4** were grown at −25 °C by layering a saturated DME solution of **2-K$_{DME}$** with $(Me_3Si)_2O$. X-ray diffraction study for **4** revealed cocrystallization of the two enantiomers of **4** in the asymmetric unit (Figure 7b). The Ce(1)—O(4) bond lengths (2.112(7) and 2.146(6) Å) are shorter than the Ce—O$_{TriNOx}$ distances measured in **2-M$_{solv}$** and **3** (Table 1) but consistent with reported Ce^{IV}—O$_{siloxide}$ distances.[23] The positional disorder of the TriNOx fragments in **4** precludes detailed examination of their geometrical parameters.

Mindiola and co-workers hypothesized the formation of a putative Sc═O complex in the reaction between the Sc═P complex and benzophenone.[8] We found that the related aza-Wittig reaction between the *in situ* generated **2-Rb$_{DME}$** complex and benzophenone yielded a thermally stable Ce(IV)–oxo complex **5** (Figure 7a). The formation of the imine byproduct in the reaction mixture, $Ph_2C{=}N(3,5\text{-}(CF_3)_2C_6H_3)$, was proven by ^{1}H and ^{19}F NMR spectroscopy, mass spectrometry, and X-ray diffraction studies (Figure S5). Compound **5** precipitated from the reaction solution as a moisture and air tolerant yellow solid in 55% yield based on the starting material, anilide **1**. X-ray quality crystals of **5** were grown from a hot THF solution. A structural study for **5** showed the aggregation of the (TriNOx)Ce═O moieties with the rubidium cations forming the supramolecular tetrameric units **(5)$_4$** (Figure 7c,d). The resulting aggregation motif where the central $Ce_4O_4Rb_4$ cluster is sterically protected by TriNOx ligand frameworks

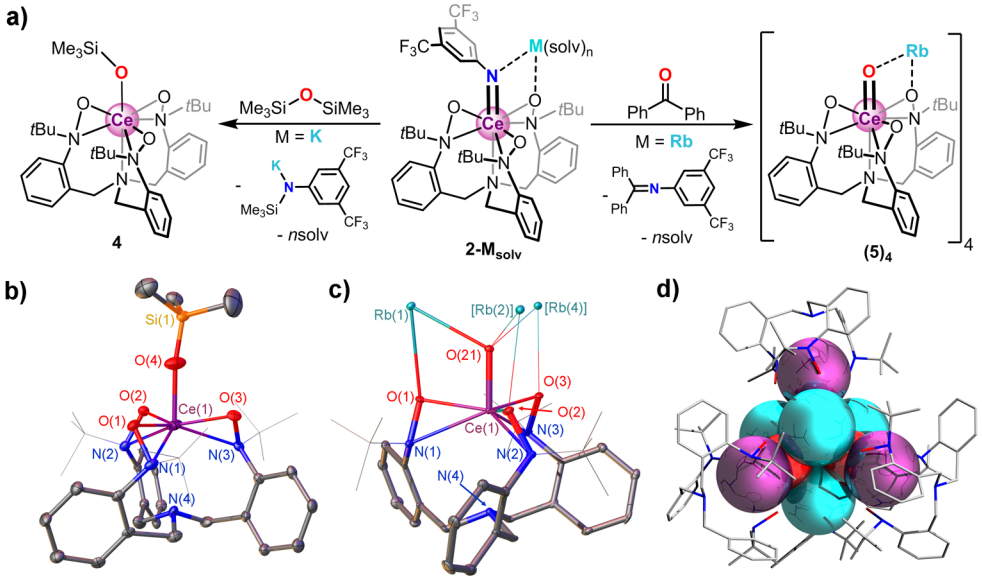

Figure 7. Preparation of **4** and **(5)$_4$** (a); thermal ellipsoid plots for **4** (only one of the enantiomers is shown) and for the monomeric unit of **(5)$_4$** shown at the 30% probability level (b and c); and tetrameric aggregate **(5)$_4$**·8THF (d, the central $Ce_4O_4Rb_4$ core is shown using a space-filling model). Hydrogen atoms and interstitial THF molecules have been omitted for clarity.

DOI: 10.1021/jacs.6b12369
J. Am. Chem. Soc. 2017, 139, 2435–2442

provides thermal, moisture, and air stability of the reactive Ce^{IV}=O units within $(\mathbf{5})_4$. The Rb—$O_{Ce=O}$ bond distances (2.745(5)−2.804(4) Å) are shorter than the Rb—O_{TriNOx} distances (2.850(4)−2.910(5) Å) because of stronger electrostatic interactions. The formation of a similar cubane-type Rb_4O_4 core was previously observed for rubidium alkoxides and anionic $TEMPO^-$ salts.[24] The Ce=O_{oxo} bond lengths range from 1.887(4) to 1.902(4) Å. These values are significantly shorter than the single Ce—O bonds measured in cerium oxide clusters (above 2.20 Å) that contain Ce—O—Ce linkages[25] but fall in the range measured for dimeric, alkali metal ion capped cerium oxo complexes (1.862(2)−1.948(4) Å).[26] The Ce=O bond lengths in $(\mathbf{5})_4$ are also similar to the Ce=O distance, reported for complex **III** (1.902(5) Å, Scheme 1).[15] The Ce=O_{oxo} bond lengths in **5** are longer than that measured in complex **II** (1.857(3) Å)[12] and that predicted for Cp_2Ce=O (1.814 Å)[27] but substantially shorter than that in the sodium capped **II** (1.953(4) Å).[13]

CONCLUSION

We have synthesized and characterized a series of alkali metal capped Ce(IV)−imido complexes. Detailed spectroscopic, electrochemical, and structural investigations coupled with DFT studies revealed shortening of the Ce=N bond upon increasing the size of coordinated alkali metal cations. Trapping of an alkali metal countercation by the 2.2.2-cryptand cavity allowed access to the first example of a terminal Ce(IV)−imido complex with the shortest known Ce—N bond length of 2.077(3) Å. Significant cerium 5d orbital contribution to the Ce=N bond was observed for imido complexes according to DFT calculations. The cerium 4f orbital contribution to bonding increases with decreasing Ce=N bond length across the series. Finally, reactivity studies confirmed the strong nucleophilicity of the imido fragment. These studies culminated in the isolation of a rare Ce(IV)−oxo complex stabilized by supramolecular aggregation with alkali metal ions. The presented work demonstrates prospective directions for the stabilization of elusive RE=E units. Additionally, this work provides further inspiration for the development of the chemistry of rare-earth multiple bonds and exploration of their unusual and promising reactivity toward different substrates.

ASSOCIATED CONTENT

Supporting Information

The Supporting Information is available free of charge on the ACS Publications website at DOI: 10.1021/jacs.6b12369.

Figures S1−S34 and Tables S1−S7, details of experimental procedures, structural and computational investigations, and multinuclear NMR and UV−vis spectra (PDF)

X-ray crystallographic data for **2-M$_{solv}$**, **3**−**5**, and Ph_2C=N(3,5-$(CF_3)_2C_6H_3$) (CIF)

AUTHOR INFORMATION

Corresponding Author

*schelter@sas.upenn.edu

ORCID

Eric J. Schelter: 0000-0002-8143-6206

Notes

The authors declare no competing financial interest.

ACKNOWLEDGMENTS

We thank the National Science Foundation (CHE-1362854) and University of Pennsylvania for financial support of this work. This work used the Extreme Science and Engineering Discovery Environment (XSEDE), which is supported by U.S. NSF Grant Number OCI-1053575. L.A.S. thanks the NSF Graduate Research Fellowship program for support. We are also grateful to Y. Qiao and Dr. H. Fang (University of Pennsylvania) for helpful discussion.

REFERENCES

(1) Nugent, W. A.; Mayer, J. M. *Metal-Ligand Multiple Bonds*; Wiley-Interscience: New York, 1988.

(2) (a) Kriegel, B. M.; Bergman, R. G.; Arnold, J. *J. Am. Chem. Soc.* **2016**, *138*, 52. (b) Walsh, P. J.; Hollander, F. J.; Bergman, R. G. *J. Am. Chem. Soc.* **1988**, *110*, 8729. (c) Hazari, N.; Mountford, P. *Acc. Chem. Res.* **2005**, *38*, 839. (d) Burdett, K. A.; Harris, L. D.; Margl, P.; Maughon, B. R.; Mokhtar-Zadeh, T.; Saucier, P. C.; Wasserman, E. P. *Organometallics* **2004**, *23*, 2027. (e) Fürstner, A.; Thiel, O. R. *J. Org. Chem.* **2000**, *65*, 1738. (f) Cummins, C. C.; Baxter, S. M.; Wolczanski, P. T. *J. Am. Chem. Soc.* **1988**, *110*, 8731. (g) Schaller, C. P.; Wolczanski, P. T. *Inorg. Chem.* **1993**, *32*, 131.

(3) (a) Hayton, T. M. *Chem. Commun.* **2013**, *49*, 2956. (b) Ma, G.; Ferguson, M. J.; McDonald, R.; Cavell, R. G. *Inorg. Chem.* **2011**, *50*, 6500. (c) Smiles, D. E.; Wu, G.; Kaltsoyannis, N.; Hayton, T. W. *Chem. Sci.* **2015**, *6*, 3891. (d) Anderson, N. H.; Yin, H.; Kiernicki, J. J.; Fanwick, P. E.; Schelter, E. J.; Bart, S. C. *Angew. Chem., Int. Ed.* **2015**, *54*, 9386. (e) Evans, W. J.; Kozimor, S. A.; Ziller, J. W. *Science* **2005**, *309*, 1835. (f) Mullane, K. C.; Lewis, A. J.; Yin, H.; Carroll, P. J.; Schelter, E. J. *Inorg. Chem.* **2014**, *53*, 9129. (g) Lewis, A. J.; Carroll, P. J.; Schelter, E. J. *J. Am. Chem. Soc.* **2013**, *135*, 511. (h) King, D. M.; Tuna, F.; McInnes, E. J. L.; McMaster, J.; Lewis, W.; Blake, A. J.; Liddle, S. T. *Nat. Chem.* **2013**, *5*, 482. (i) Anderson, N. H.; Odoh, S. O.; Yao, Y.; Williams, U. J.; Schaefer, B. A.; Kiernicki, J. J.; Lewis, A. J.; Goshert, M. D.; Fanwick, P. E.; Schelter, E. J.; Walensky, J. R.; Gagliardi, L.; Bart, S. C. *Nat. Chem.* **2014**, *6*, 919. (j) Behrle, A. C.; Castro, L.; Maron, L.; Walensky, J. R. *J. Am. Chem. Soc.* **2015**, *137*, 14846. (k) Andrez, J.; Pécaut, J.; Scopelliti, R.; Kefalidis, C. E.; Maron, L.; Rosenzweig, M. W.; Meyer, K.; Mazzanti, M. *Chem. Sci.* **2016**, *7*, 5846.

(4) (a) Raymond, K. N.; Eigenbrot, C. W., Jr. *Acc. Chem. Res.* **1980**, *13*, 276. (b) Summerscales, O. T.; Gordon, J. C. *RSC Adv.* **2013**, *3*, 6682. (c) Masuda, J. D.; Jantunen, K. C.; Ozerov, O. V.; Noonan, K. J. T.; Gates, D. P.; Scott, B. L.; Kiplinger, J. L. *J. Am. Chem. Soc.* **2008**, *130*, 2408. (d) Scott, J.; Fan, H.; Wicker, B. F.; Fout, A. R.; Baik, M.-H.; Mindiola, D. J. *J. Am. Chem. Soc.* **2008**, *130*, 14438. (e) Gordon, J. C.; Giesbrecht, G. R.; Clark, D. L.; Hay, P. J.; Keogh, D. W.; Poli, R.; Scott, B. L.; Watkin, J. G. *Organometallics* **2002**, *21*, 4726. (f) Chan, H.-S.; Li, H.-W.; Xi, Z. *Chem. Commun.* **2002**, 652.

(5) Giesbrecht, G. R.; Gordon, J. C. *Dalton Trans.* **2004**, *16*, 2387.

(6) Scott, J.; Basuli, F.; Fout, A. R.; Huffman, J. C.; Mindiola, D. J. *Angew. Chem., Int. Ed.* **2008**, *47*, 8502.

(7) Lu, E.; Li, Y.; Chen, Y. *Chem. Commun.* **2010**, *46*, 4469.

(8) Wicker, B. F.; Scott, J.; Andino, J. G.; Gao, X.; Park, H.; Pink, M.; Mindiola, D. J. *J. Am. Chem. Soc.* **2010**, *132*, 3691.

(9) Schädle, D.; Meerman-Zimmerman, M.; Schädle, C.; Maichle-Mössmer, C.; Anwander, R. *Eur. J. Inorg. Chem.* **2015**, *2015*, 1334.

(10) Löble, M. W.; Keith, J. M.; Altman, A. B.; Stieber, S. C. E.; Batista, E. R.; Boland, K. S.; Conradson, S. D.; Clark, D. L.; Pacheco, J. L.; Kozimor, S. A.; Martin, R. L.; Minasian, S. G.; Olson, A. C.; Scott, B. L.; Shuh, D. K.; Tyliszczak, T.; Wilkerson, M. P.; Zehnder, R. A. *J. Am. Chem. Soc.* **2015**, *137*, 2506.

(11) (a) Smiles, D. E.; Wu, G.; Hayton, T. W. *J. Am. Chem. Soc.* **2014**, *136*, 96. (b) Arney, D. S. J.; Burns, C. J. *J. Am. Chem. Soc.* **1993**, *115*, 9840. (c) Jilek, R. E.; Spencer, L. P.; Kuiper, D. L.; Scott, B. L.; Williams, U. J.; Kikkawa, J. M.; Schelter, E. J.; Boncella, J. M. *Inorg. Chem.* **2011**, *50*, 4235. (d) Schmidt, A.-C.; Heinemann, F. W.; Maron,

DOI: 10.1021/jacs.6b12369
J. Am. Chem. Soc. 2017, 139, 2435−2442

L.; Meyer, K. *Inorg. Chem.* **2014**, *53*, 13142. (e) Diaconescu, P. L.; Arnold, P. L.; Baker, T. A.; Mindiola, D. J.; Cummins, C. C. *J. Am. Chem. Soc.* **2000**, *122*, 6108. (f) Jilek, R. E.; Tomson, N. C.; Shook, R. L.; Scott, B. L.; Boncella, J. M. *Inorg. Chem.* **2014**, *53*, 9818.
(12) So, Y.-M.; Wang, G.-C.; Li, Y.; Sung, H. H.-Y.; Williams, I. D.; Lin, Z.; Leung, W.-H. *Angew. Chem., Int. Ed.* **2014**, *53*, 1626.
(13) So, Y.-M.; Li, Y.; Au-Yeung, K.-C.; Wang, G.-C.; Wong, K.-L.; Sung, H. H. Y.; Arnold, P. L.; Williams, I. D.; Lin, Z.; Leung, W.-H. *Inorg. Chem.* **2016**, *55*, 10003.
(14) Damon, P. L.; Wu, G.; Kaltsoyannis, N.; Hayton, T. W. *J. Am. Chem. Soc.* **2016**, *138*, 12743.
(15) Gregson, M.; Lu, E.; McMaster, J.; Lewis, W.; Blake, A. J.; Liddle, S. T. *Angew. Chem., Int. Ed.* **2013**, *52*, 13016.
(16) Levine, D. S.; Tilley, T. D.; Andersen, R. A. *Organometallics* **2017**, *36*, 80.
(17) Solola, L. A.; Zabula, A. V.; Dorfner, W. L.; Manor, B. C.; Carroll, P. J.; Schelter, E. J. *J. Am. Chem. Soc.* **2016**, *138*, 6928.
(18) (a) Bogart, J. A.; Lippincott, C. A.; Carroll, P. J.; Schelter, E. J. *Angew. Chem., Int. Ed.* **2015**, *54*, 8222. (b) Bogart, J. A.; Lippincott, C. A.; Carroll, P. J.; Booth, C. H.; Schelter, E. J. *Chem. - Eur. J.* **2015**, *21*, 17850.
(19) Zabula, A. V.; Petrukhina, M. A. *Adv. Organomet. Chem.* **2013**, *61*, 375.
(20) Shannon, R. D. *Acta Crystallogr., Sect. A: Cryst. Phys., Diffr., Theor. Gen. Crystallogr.* **1976**, *32*, 751.
(21) Kauffmann, E.; Dye, J. L.; Lehn, J.-M.; Popov, A. I. *J. Am. Chem. Soc.* **1980**, *102*, 2274.
(22) (a) Bogart, J. A.; Lewis, A. J.; Medling, S. A.; Piro, N. A.; Carroll, P. J.; Booth, C. H.; Schelter, E. J. *Inorg. Chem.* **2013**, *52*, 11600. (b) Dorfner, W. L.; Carroll, P. J.; Schelter, E. J. *Dalton Trans.* **2014**, *43*, 6300. (c) Schneider, D.; Spallek, T.; Maichle-Mössmer, C.; Törnroos, K. W.; Anwander, R. *Chem. Commun.* **2014**, *50*, 14763.
(23) (a) Gradeff, P. S.; Yunlu, K.; Gleizes, A.; Galy, J. *Polyhedron* **1989**, *8*, 1001. (b) Wang, G.-C.; So, Y.-M.; Wong, K.-L.; Au-Yeung, K.-C.; Sung, H. H.-Y.; Williams, I. D.; Leung, W.-H. *Chem. - Eur. J.* **2015**, *21*, 16126.
(24) (a) Chisholm, M. H.; Drake, S. R.; Naiini, A. A.; Streib, W. E. *Polyhedron* **1991**, *10*, 337. (b) Balloch, L.; Drummond, A. M.; García-Álvarez, P.; Graham, D. V.; Kennedy, A. R.; Klett, J.; Mulvey, R. E.; O'Hara, C. T.; Rodger, P. J. A.; Rushworth, I. D. *Inorg. Chem.* **2009**, *48*, 6934.
(25) (a) Malaestean, I. L.; Ellern, A.; Baca, S.; Kögerler, P. *Chem. Commun.* **2012**, *48*, 1499. (b) Mathey, L.; Paul, M.; Copéret, C.; Tsurugi, H.; Mashima, K. *Chem. - Eur. J.* **2015**, *21*, 13454.
(26) Coles, M. P.; Hitchcock, P. B.; Khvostov, A. V.; Lappert, M. F.; Li, Z.; Protchenko, A. V. *Dalton Trans.* **2010**, *39*, 6780.
(27) Clark, D. L.; Gordon, J. C.; Hay, P. J.; Poli, R. *Organometallics* **2005**, *24*, 5747.

DOI: 10.1021/jacs.6b12369
J. Am. Chem. Soc. 2017, 139, 2435−2442